Wearable Aperture-Coupled Shorted Solar Patch Antenna for Remote Tracking and Monitoring Applications

F. Declercq*, A. Georgiadis†, H. Rogier*
*Ghent University, Department of Information Technology (INTEC)
9000, Ghent, Belgium
fdclercq@intec.ugent.be
†Centre Tecnològic de telecommunicacions de Catalunya (CTTC)
08860, Castelldefels, Spain
ageorgiadis@cttc.es

***Abstract*—This paper presents the design and characterization of a compact wearable aperture-coupled shorted patch antenna combined with flexible solar cells covering the 902-928 MHz ISM band. The antenna is constructed solely out of flexible foam and textile materials. The parallel connected amorphous silicon (a:Si-H) solar cells are able to deliver a maximum DC power output of about 96 mW. Combining solar cells with a shorted patch antenna allows a simple realization of the DC output wire connections without disturbing the antenna's radiation characteristics. A measured on-body antenna gain and bandwidth of about 1.6 dBi and 63 MHz are realized, respectively.**

I. Introduction

Wearable computing and body-centric wireless communication has received a vast amount of attention, especially for the health care or protective clothing industry, where real-time bio-monitoring and tracking of persons is of vital importance. These autonomous wearable textile systems must be lightweight, flexible and have a small surface coverage to realize an unobtrusive integration. Unlike the computational hardware, which has decreased in size and improved in power efficiency, the power system itself has remained rather bulky and inconvenient for wearable applications. Therefore, environmental power harvesting methods will play a key-role in the proliferation of wearable textile systems. Several approaches for energy harvesting from the environment or from the user's activities have been studied [1], [2], [3]:

- Solar energy
- Vibration-to-electricity
- Kinetic energy from walking or breathing
- Thermal energy from body heat (Thermoelectric generators)

These methods could serve as an additional power supply charging the flexible batteries or eliminate the need for batteries.

The development of flexible amorphous silicon (a-Si:H) solar cells on a flexible thin film polymer substrate resulted in an eco-friendly, reliable and low-cost power supply suitable for integration into clothing [4]. These solar cells combined with integrated wearable antennas in the garment, tend to consume quite some space, and, as a result, the available surface area on the garment is becoming limited. As presented in [5], [6] the solar cells can be glued on top or placed next to the radiating patch without disturbing its radiation function as long as the radiating edges of the patch remain free. In [7] a reflectarray antenna was combined with a solar cell array. In [8] the conductive backside contacts of the solar cell are adopted as the radiating patch, realizing a higher level of integration since both the RF and DC functionality are merged together. Other work presented in [9], [10] also reported a more complete integration by cutting out slot structures in amorphous silicon solar cells which are then adopted as slot antennas.

In this work we present a wearable aperture-coupled shorted solar patch antenna for communication in the 902 - 928 MHz UHF band. This novel design uses the same area for RF radiation as for DC power generation, minimizing the overall size of the body-centric wireless communication system. Moreover, the shorting wall introduces a simple realization of routing the DC output connections of the solar cells to the circuitry without disturbing the radiation performance of the antenna. In Section II the antenna topology and the design in CST Microwave Studio is discussed. The integration of the a:Si-H solar cells is described in Section III-A, while Section III-B describes the DC characterization of the solar cells. Finally, the measurements are discussed and compared with the simulations in Section IV.

II. Configuration and Design Shorted Solar Patch Antenna

The geometry of the aperture-coupled shorted patch antenna is depicted in Fig. 1. An aperture coupling feeding technique was introduced to avoid a fragile soldered probe feed connection and thereby improving the flexibility of the overall design. Given the large wavelength at the frequency of operation a shorted patch antenna was selected, resulting in a more compact antenna compared to conventional $\lambda/2$ antennas, making it a suitable antenna topology for wearable applications. Also

the presence of a ground plane minimizes the bulk power absorption in the human body [11]. An H-shaped coupling slot is introduced to further improve the coupling performance of the design and this to minimize the backward radiation into the human body [12]. The antenna height was kept small to have a low-profile design while providing a sufficiently large antenna volume, yielding good bandwidth performance to account for fabrication inaccuracies, variations in material parameters and frequency de-tuning caused by the proximity of the human body.

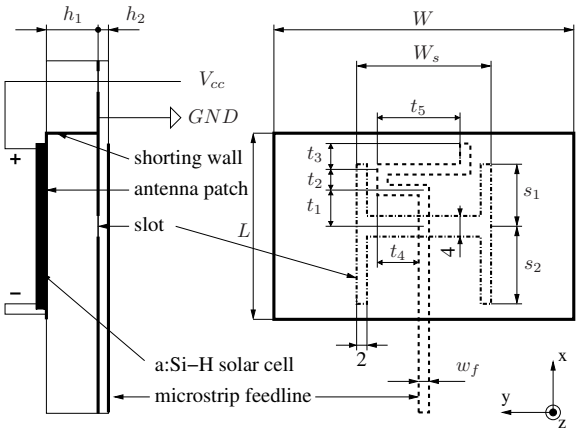

Fig. 1. Geometry of the aperture-coupled shorted solar patch antenna with dimensions in mm.

A. Antenna Materials

The antenna substrate is a flexible polyurethane protective foam, typically used in professional garments with a thickness h_1 = 11 mm, a permittivity ϵ_r = 1.16 and a loss tangent, $\tan\delta$ = 0.010. The feed substrate is constructed by assembling two aramid textile layers typically used as outer layer in firefighter jackets, resulting in a thickness h_2 of 0.95 mm, a permittivity of 1.97 and a $tan\delta$ = 0.02. The conductive patch and ground plane are made out of Flectron, a copper coated nylon fabric with a surface resistivity R_s = 0.10 Ω/sq. The microstrip feed line is constructed using copper foil. The ground plane, the antenna patch, the microstrip feed line and the aramid layers are assembled together by means of an adhesive sheet. The radiating patch with length L and width W is shorted to the ground plane by a conducting wall constructed out of Flectron. The shorting wall is constructed by folding the patch, inserting it through the antenna substrate and taping it to the ground plane using conductive tape. The H-shaped slot with dimensions s_1, s_2 and W_s, which couples the electromagnetic energy from the 50 Ω microstrip line into the shorted patch, is centered underneath the patch. The footprint of the microstrip feed line is minimized by meandering the stub with dimensions t_1, t_2, t_3, t_4 and t_5.

B. Antenna Design

The antenna was designed using the time domain solver of CST Microwave Studio. During the design process, the microstrip feed line in the simulation model was not meandered, allowing us to impose a magnetic symmetry condition in the XZ-plane, yielding faster simulation time. The conductive Flectron textile layer with a thickness of 150 μm was defined as a lossy metal with an effective bulk conductivity calculated by $\sigma = \pi f \mu_0 / R_s^2 = 361230\ S/m$, wherein f = 915 MHz is the frequency of operation and $\mu_0 = 4\pi \times 10^{-7}$ H/m is the magnetic permeability. During the design process, the antenna dimensions L, W, s_1, s_2, W_s and t_5 were optimized to meet the specified bandwidth requirement of $|S_{11}| \leq -10\ dB$ in the frequency range from 902 MHz to 928 MHz. The resulting antenna dimensions are given in Table I. The total ground plane size is about 120 mm x 120 mm. Note that the simulation model did not include the SMA connector.

TABLE I
ANTENNA DIMENSIONS

Patch [mm]	Slot [mm]	Stub [mm]
L, W	s_1, s_2, W_s	t_1,t_2,t_3,t_4,t_5
62,80	24,28,36	11,12,10,12,24
Feed Line [mm]	w_f	3

III. SOLAR CELL INTEGRATION AND DC CHARACTERISTICS

A. Solar Cell Integration

The a-Si:H solar cell is a multilayered structure and consist of a flexible polyimide carrier, an aluminum layer and a p-i-n silicon layer that is located between two transparent conductive zinc oxide (ZnO) layers. The total thickness of the solar cell is about 200 μm and since the wavelength is relatively large at the frequency of operation, the influence of the solar cell on the antenna performance is negligible. The size of the solar cell aperture is 50 mm x 37 mm yielding an active area of 18.5 cm^2 for one solar cell. Fig. 2 depicts the antenna with two solar cells glued on top of the Flectron patch and Fig. 3 shows us the meandered microstrip feed line. The solar cells are placed in such a manner that the edge opposite to the shorting wall of the shorted aperture-coupled patch antenna is not covered, since the fringing electric fields at this radiating edge are responsible for the antenna radiation [1]. The DC- contact of the solar cell is soldered onto the patch using a copper wire, while the DC+ contact wires are routed through the substrate at the side of the shorting wall. Since the side of the shorting wall is not a radiating edge, the positive voltage DC connections will not affect the radiation characteristics of the antenna. As an example we place the solar cells in parallel. A schematic representation of two parallel connected solar cells S_1 and S_2 is depicted in Fig. 4. Considering two differently illuminated solar cells, a diode D connected in series with each cell will prevent the flow of reverse current. The total open circuit output voltage will be equal to the largest of both voltages and the short circuit current will be equal to the sum of all short circuit currents [13]. Schottky diodes are chosen since the voltage drop across the diodes is smaller compared to conventional diodes. The regulator circuit providing a constant

voltage supply V_{out} will be positioned below the ground plane to minimize the coupling between the circuitry and the patch antenna. Since the solar cells are connected to the patch and antenna ground plane, a series inductor L_1 and RF-decoupling capacitor C_1 are introduced.

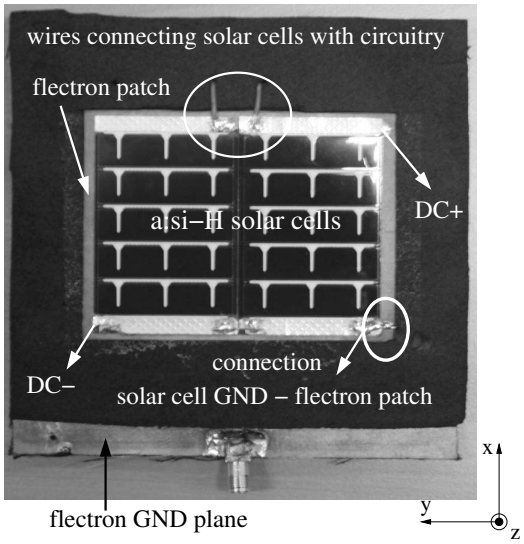

Fig. 2. Picture of the antenna with two solar cells glued on top (parallel configuration).

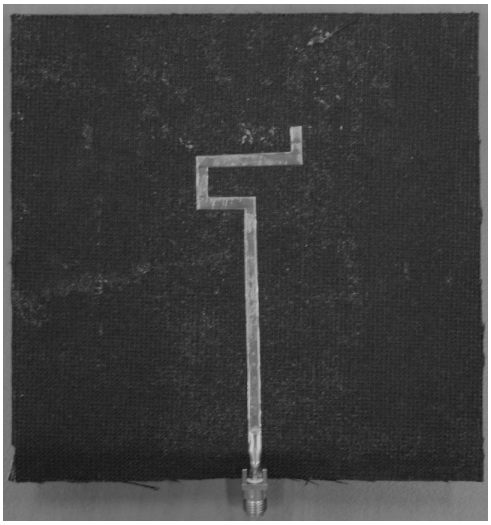

Fig. 3. Picture of the meandered microstrip line feeding the aperture-coupled shorted patch antenna.

B. Solar Cell DC Properties

The solar cell's DC I-V characteristic was measured using a solar simulator with an illumination of 100 mW/cm^2, representing sunlight directly overhead and a turbidity free sky. The measurement results are depicted in Fig. 5. The measured open circuit voltage V_{oc} and short circuit current I_{sc} are 4.23 V and 26.25 mA, respectively. The maximum power point occurs at 3 V and 19.1 mA, resulting in a maximum deliverable power

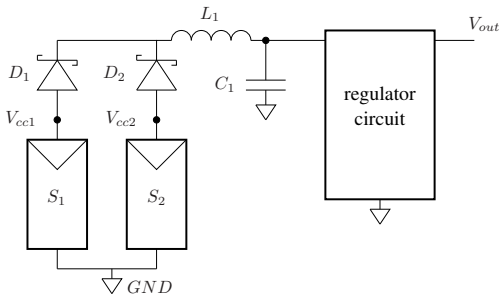

Fig. 4. Schematic representation parallel connected solar cells S_1 and S_2.

of 57.3 mW. Including the blocking diodes with a forward voltage of 500 mV reduces the maximum deliverable power to 48 mW per solar cell. Considering the parallel connection of the two solar cells as depicted in Fig. 4, a maximum DC output power of about 96 mW can be obtained. In a real-life application the solar cell will not be illuminated as strongly as with the solar simulator. Also the position of the antenna in the clothing will be as such that the sunlight will not be directly overhead, resulting in a lower DC power output.

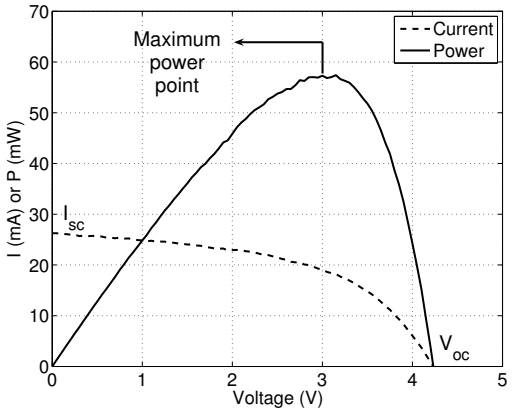

Fig. 5. I-V characteristic of the solar cell.

IV. Measurement and Simulation Results

The reflection coefficients of the antenna were measured using the N5242A PNA-x from Agilent Technologies and are depicted in Fig. 6. The simulated bandwidth and the measured bandwidth of our antenna without solar cells is 48 MHz. Note that the simulated results are from the CST model with a meandered microstrip feed line and hence without the magnetic symmetry condition in the XZ-plane, since gain and bandwidth is affected by the size of the ground plane. When integrating the solar cells on top of the patch we observe a slightly larger bandwidth because of the additional losses caused by the presence of the solar cell. For the on-body measurement, the antenna was located on the chest and this to minimize the bending of the antenna. The measured on-body bandwidth has increased to 64 MHz caused by the additional losses introduced by placing the antenna in proximity of the

human body. This proves that the antenna still operates in the proximity of the human body. The gain measurements were performed inside an anechoic chamber using an orbit/FR positioning system combined with the PNA-x measurement system. The radiation pattern in the XZ as well as in the YZ-plane were measured for the antenna with and without solar cells. For the case with the solar cells, the DC+ connection wires were also included in the measurement. The measured and simulated free space gain at 915 MHz in the XZ-plane and YZ-plane are depicted in Fig. 7 and Fig. 8, respectively.

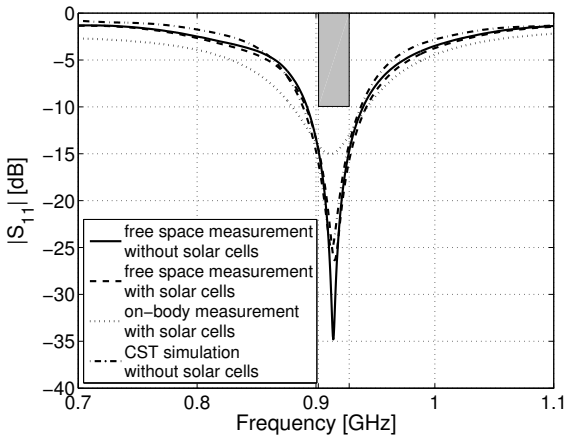

Fig. 6. Measured and simulated reflection coefficients of the wearable aperture-coupled shorted patch antenna.

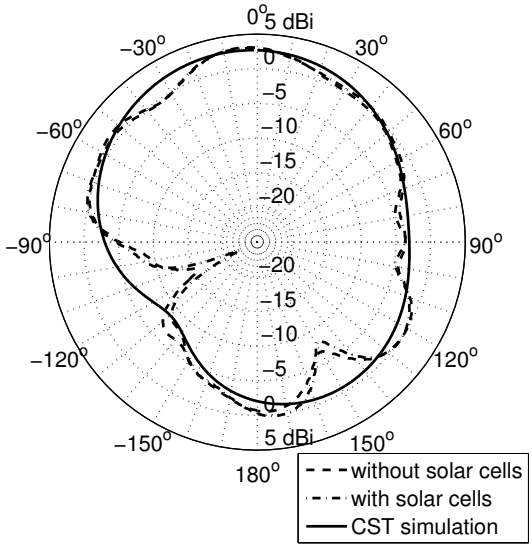

Fig. 7. Measured and simulated gains in the XZ-plane of the wearable aperture-coupled shorted patch antenna at 915 MHz.

A very good agreement is observed between the measured and simulated results. From these measurements we can conclude that the solar cells combined with the DC+ connection wires have a minor influence on the radiation behavior of the antenna. A maximum measured and simulated gain of about 3 dBi and 2.7 dBi is observed, respectively. For the on-body

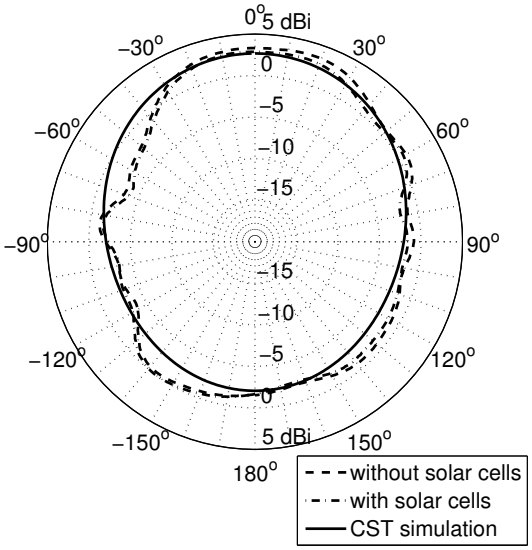

Fig. 8. Measured and simulated gains in the YZ-plane of the wearable aperture-coupled shorted patch antenna at 915 MHz.

gain measurement, the antenna was located on the chest and great care was taken with the alignment between the antennas in the anechoic chamber. The on-body gain measurement result in the YZ-plane is depicted in Fig. 9 and a maximum gain of 1.6 dBi is observed.

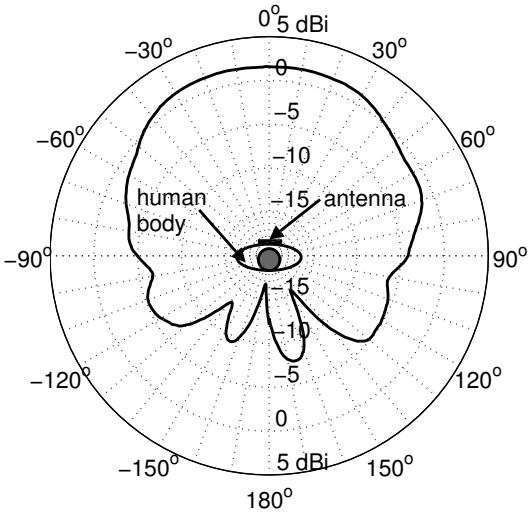

Fig. 9. Measured on-body gain of the wearable aperture-coupled shorted patch antenna with solar cells at 915 MHz.

V. Conclusions

A wearable aperture-coupled shorted patch antenna for the 902 - 928 MHz has been designed and successively combined with amorphous silicon solar cells, minimizing the required surface area of the wireless body-centric communication system. The parallel connected solar cells are able to deliver up to 96 mW of DC output power. It is shown that the effect of the solar cells on the antenna characteristics is minimal given

the large wavelength at 915 MHz. Also the shortening wall of the antenna allows an easy DC connection without affecting the antenna characteristics.

ACKNOWLEDGEMENTS

This research was accomplished during a Short Term Scientific Mission (COST-STSM-IC0803-6338) in the framework of COST Action IC0803-RF / Microwave Communication Subsystems for Emerging Wireless Technologies. The work of A. Georgiadis was also supported by the Spanish Ministry of Science and Innovation project TEC2008-02685/TEC, and PTQ-06-02-0555, and by Marie Curie project SWAP, FP7-PEOPLE-2009-IAPP 251557.

REFERENCES

[1] T. Starner, "Human-powered wearable computing," *IBM Systems Journal*, vol. 35, no. 3-4, pp. 541–550, 1996.

[2] S. Roundy, B. P. Otis, Y.-H. Chee, J. M. Rabaey, and P. Wright, "A 1.9 GHz RF transmit beacon using environmentally scavenged energy," in *Dig. IEEE Int. Symposium on Low Power Elec. and Devices, Seoul, Korea*, 2003.

[3] A. Rida, L. Yang, and M. Tentzeris, *RFID-Enabled sensor design and applications*. Norwood, MA, USA: Artech House, 2010.

[4] B. S. Markus and H. W. Jürgen, "Flexible solar cells for clothing," *Materials Today*, vol. 9, no. 6, pp. 42–50, 2006.

[5] M. Tanaka, Y. Suzuki, K. Araki, and R. Suzuki, "Microstrip antenna with solar cells for microsatellites," *IEE Electronics Letters*, vol. 31, no. 1, pp. 5–6, Jan. 1995.

[6] S. Vaccaro, P. Torres, J. Mosig, A. Shah, J.-F. Zurcher, A. Skrivervik, F. Gardiol, P. de Maagt, and L. Gerlach, "Integrated solar panel antennas," *IEE Electronics Letters*, vol. 36, no. 5, pp. 390–391, Mar. 2000.

[7] M. Zawadzki and J. Huang, "Integrated RF antenna and solar array for spacecraft application," in *Phased Array Systems and Technology, 2000. Proceedings. 2000 IEEE International Conference on*, Dana Point, CA, May 2000, pp. 239–242.

[8] M. Danesh, J. R. Long, and M. Simeoni, "Small-area solar antenna for low-power UWB transceivers," in *Antennas and Propagation, 2009. EuCAP 2009. 4th European Conference on*, Barcelona, Spain, Apr. 12-16, 2010, pp. 1–4.

[9] S. Vaccaro, J. Mosig, and P. de Maagt, "Two advanced solar antenna "SOLANT" designs for sattelite and terrestrial communications," *IEEE Trans. Antennas Propag.*, vol. 51, no. 8, pp. 2028–2034, Aug. 2003.

[10] S. Shynu, M. Roo Ons, M. Ammann, S. McCormack, and B. Norton, "Dual band a-Si:H solar-slot antenna for 2.4/5.2 GHz WLAN applications," in *Antennas and Propagation, 2009. EuCAP 2009. 3rd European Conference on*, Berlin, Germany, Mar. 23-27, 2009, pp. 408–410.

[11] P. Salonen, L. Sydänheimo, M. Keskilammi, and M. Kivikoski, "A small planar inverted-F antenna for wearable applications," in *Wearable Computers, 1999. Digest of Papers. The Third International Symposium on*, Oct 1999, pp. 95–100.

[12] V. Rathi, G. Kumar, and K. Ray, "Improved coupling for aperture coupled microstrip antennas," *IEEE Trans. Antennas Propag.*, vol. 44, no. 8, pp. 1196–1198, Aug. 1996.

[13] M. Slonim and D. Shavit, "Linearization of the output characteristics of a solar cell and its application for the design and analysis of solar cell arrays," in *Energy Conversion Engineering Conference, 1997. IECEC-97., Proceedings of the 32nd Intersociety*, vol. 3, Honolulu, HI, USA, 27 Jul.-01 Aug. 1997, pp. 1934 –1938.